Journal of Research and Applications in Mechanical Engineering
ISSN: 2229-2152 (Print); 2697-424x (Online)
(2024) Vol. 12, No. 2, Paper No. JRAME-24-12-029
[DOI: 10.14456/jrame.2024.29]

Research Article

Efficiency and Control: Modelling and Validation of an Electric Fan Bus Cooling System

A. Kosin
A. Kosiyanurak
T. Sri-on
N. Pothi
J. Srisertpol*
Graduated Program in Mechatronic Engineering, School of Mechanical Engineering, Institute of Engineering, Suranaree University of Technology, Nakhon Ratchasima, 30000, Thailand

Received 27 September 2023
Revised 23 February 2024
Accepted 3 March 2024

Abstract:
The cooling systems in the majority of passenger buses typically depend on mechanical or hydraulic cooling systems. These systems utilize the engine's generated energy to function, leading to increased engine workload and higher fuel consumption. However, an electric cooling system presents the advantage of reducing the engine's workload and providing enhanced control. This paper focuses on modelling, validating, and presenting experimental results of an electric fan cooling system. Based on the accuracy assessment of the heat exchange system's mathematical model studied in this research, the evaluation was conducted using the Root Mean Square Error (RMSE) of the mathematical model's response compared to the actual system response obtained from experiments. It was observed that the RMSE of the outlet air temperature is 0.50, and the RMSE of the cooling water temperature at the water outlet is 0.21. Therefore, it can be concluded that the estimated mathematical model is accurate and closely approximates the real system. Additionally, it aims to utilize the benefits of the mathematical model to design a control system specifically tailored to the engine's operating conditions.

Keywords: *Electric fan cooling system, Heat exchanger, MATLAB/Simulink*

1. Introduction

Currently, electric vehicles (EVs) for mass transportation have gained significant attention in the automotive industry, surpassing the production of internal combustion engine (ICE) vehicles [1]. This is because ICE engines require fossil fuels as an energy source, resulting in energy losses through incomplete combustion (exhaust gas), leading to environmental pollution [1, 2]. Additionally, energy losses occur from the cooling system and internal friction, reducing the engine's overall efficiency to approximately 34-38% [3]. Consequently, automotive manufacturers have been modifying the powertrain components from ICE engines to efficient electric motors, with lower maintenance costs, to meet increasing consumer demands. The conventional cooling system of the engine consists of fans and water pumps that require power from the engine to operate. These components work to drive air through the radiator and circulate coolant within the system. As a result, the engine experiences an increased load for its operation. Additionally, there is a thermostat valve that regulates the flow area of the coolant to adjust the flow rate and control its temperature, contributing to increased engine load due to elevated pressure losses in the cooling circuit [4, 5]. Usually, such systems are designed to operate under the worst conditions, and they cannot maintain the higher efficiency of the system. However, advancements have led to the introduction of electrically driven fans and water pumps, providing the ability to dissipate heat from the engine based on its operating conditions. This approach has resulted in reduced fuel consumption [4] and improved engine stability [6]. Researchers [6] have proposed utilizing

* Corresponding author: J. Srisertpol
E-mail address: jiraphon@sut.ac.th

a cooling system with electrically driven water pumps and fans for a 1.4 liter engine, controlling both components to meet the conditions specified by the New European Driving Cycle (NEDC). The study shows that using electric pumps and fans can lead to a maximum reduction in fuel consumption by 1.1%, along with a decrease in hydrocarbon and carbon monoxide gas emissions by 5.3% and 6.1% [7], respectively. Moreover, the study suggests that employing an electrically driven cooling system with water pumps and fans can reduce pollutant emissions by 10% and decrease fuel consumption by 3% [7]. The ability to control the operating conditions for maximum efficiency is achieved through the design of a suitable control system tailored to the engine's operation and internal components. Researchers [8] present the use of a proportional and derivative (PD) control system to regulate the cooling system's operation, highlighting a potential reduction in fuel consumption by 1.5% for city driving conditions. Similarly, another study [9] suggests the use of a proportional and integral (PI) control system for an engine utilizing water pumps, fans, and a three-way valve to control the coolant temperature under specified conditions, achieving satisfactory and accurate results. In a different approach, researchers [10] propose using a Model Predictive Control (MPC) system for a 1.2-liter engine's cooling system. The study finds that the system can control the flow rate of coolant, leading to a reduction in power required to drive the water pump, thereby improving overall efficiency.

The system can also maintain the coolant temperature within desired limits under varying operating conditions. As mentioned above, the utilization of electrically driven water pumps and fans in the cooling system contributes to the engine's enhanced capabilities and improved performance in terms of mechanical aspects, operational stability, and a potential reduction in cost and fuel consumption.

This research study investigates and tests a water and air-based heat dissipation system, particularly the radiator, to assess the temperature response of the radiator system. The data obtained is used to estimate the parameters of the radiator system in a mathematical model. This mathematical model's results are compared and validated against the actual system's responses to confirm that the mathematical model of the heat exchange system using the radiator is accurate and suitable for future applications [9, 11-13]. This model can be effectively employed for the design of a radiator cooling system controller that is both accurate and suitable for future applications.

2. Experimental Setup

The experimental equipment utilized in this research was sourced from the cooling unit of an internal combustion engine passenger bus from Cherdchai Corporation Co., Ltd. The aim was to investigate potential applications for cooling electric passenger buses in the future. Consequently, the experimental setup for the passenger bus cooling experiment was devised with multiple components, as illustrated in Fig. 1, to replicate the heat dissipation process. This setup incorporates a hot water bath equipped with an electric heater to simulate heat generation within the system. A PID controller-managed engine water pump ensures a consistent water flow rate. The hot water generated is directed into a radiator, where it transfers heat through tubes and fins to the incoming air, assisted by three fans. To monitor and regulate temperatures within the system, various sensors are employed. Specifically, an NTC thermistor sensor is used to measure the water's temperature both as it enters and exits the radiator, while a K-type thermocouple sensor gauges the air's temperature as it enters and exits the radiator. The primary objective of this setup is to collect experimental data enabling the control of water flow rates, maintaining them at a constant level throughout testing. To manipulate the air flow rate, adjustments are made by altering fan speed or changing the number of fans in operation. In the testing phase, the temperature from the hot water bath is around 70-80 $^{\circ}$C (Studying the operating range of coolant temperature in an internal combustion engine [9]), and the water pump speed is maintained at 800 rpm, with a constant water flow rate of 0.45 kg/s. Four distinct cases are tested: Case 1, three fans are activated at 85% speed, running at 2500 rpm. Case 2, three fans are active at 60% speed, operating at 1680 rpm. Case 3 involves activating two fans at 85% speed. Case 4 features two fans operating at 60% speed.

These cases aim to observe the system's response to temperature changes in both the water and air inlet and outlet. The obtained experimental values will be compared to simulation data generated using MATLAB/Simulink. This comparison will serve to validate the Simulink model against real-world experimental results.

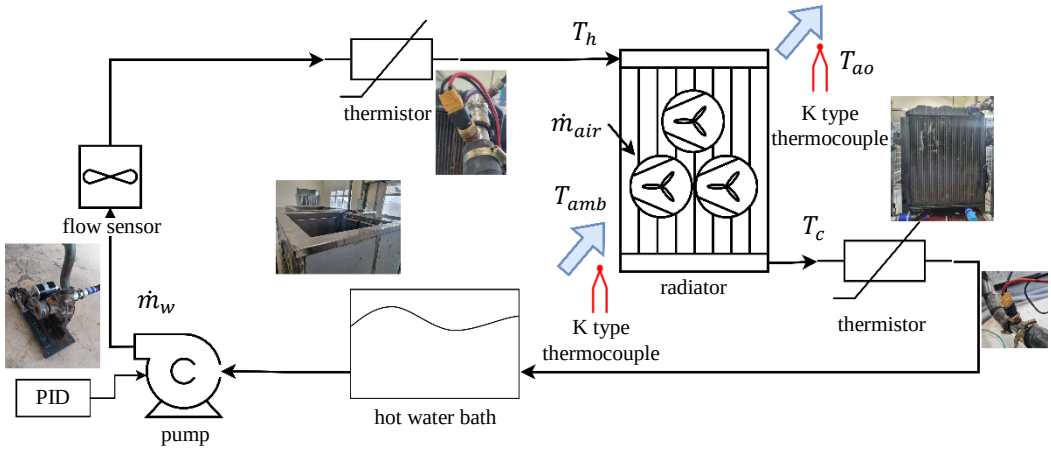

Fig. 1. The experimental setup.

3. Mathematic Model

The study explores the thermodynamic characteristics of a heat exchange system utilizing water and air within the radiator system of an internal combustion engine. In this research, mathematical models based on the energy balance within the radiator system, accounting for both the coolant water and the cooling air, are examined using Equations 1 and 2. The mass flow rates of both types of flows are presumed to vary under experimental conditions, influencing the alteration in the system's heat exchange rate represented by the term Q_{ex}, as presented in Equation 3. The investigation centers on the crossflow heat exchange apparatus in the radiator, considering the correction factor (F) that affects the heat exchange rate of the system. This leads to variations in the heat transfer coefficient in response to the heat exchange operation of the system, assessable from Equations 4 and 5. These equations are employed to estimate the temperature difference between the coolant water and the cooling air at the system's inlet and outlet positions. Moreover, the flow rate of the system flow is an additional variable impacting the observed heat exchange rate, as indicated in Equations 6, 7, and 8. Equation 9 is employed to estimate the Prandtl number, and the entire set of equations mentioned above is applied for the mathematical model approximation and the study of the thermodynamic behavior of the heat exchange system. The mass flow rate, inlet temperature, and ambient air temperature are considered as independent variables, while the outlet temperatures of the coolant water and the cooling air from the radiator are regarded as dependent variables, as shown below.

Heat balance on cooling water side

$$\rho_w \forall_{rad} c_{p,w} \frac{dT_c}{dt} = \dot{m}_w c_{p,w} T_h - Q_{ex} - \dot{m}_w c_{p,w} T_c + \dot{m}_{res} c_{p,w} T_{c,t=0} \tag{1}$$

Heat balance on cooling air side

$$\rho_a \forall_{air} c_{p,a} \frac{dT_{ao}}{dt} = \dot{m}_{air} c_{p,air} T_{amb} - Q_{ex} - \dot{m}_{air} c_{p,air} T_{ao} + \dot{m}_{air,eff} c_{p,air} T_{amb} \tag{2}$$

heat exchange rate

$$Q_{ex} = UA\Delta T_{LMD} F \tag{3}$$

The overall heat transfer coefficient (U)

$$U = \frac{1}{h_i} + \frac{L}{k} + \frac{1}{h_o} \tag{4}$$

Log mean temperature difference

$$\Delta T_{LMT} = \frac{(T_h - T_{ao}) - (T_c - T_{amb})}{\ln(\frac{T_h - T_{ao}}{T_c - T_{amb}})} \quad (5)$$

Nusselt number (NU)

$$Nu = \frac{hD_h}{k} \quad (6)$$

Nusselt number for Turbulent correlation

$$Nu = 0.023 \times \mathrm{Re}^{0.8} \times \mathrm{Pr}^{1/3} \quad (7)$$

Nusselt number for Laminar correlation

$$Nu = 3.66 \times \left(\frac{\mathrm{Re} \times \mathrm{Pr}}{1.07} \right)^{1/3} \quad (8)$$

Prandtl number (Pr)

$$Pr = \frac{c_p \mu}{k} \quad (9)$$

4. Experimental and Simulation Results

4.1 Static Performance

Table 1: Result of parameter estimation.

case no.	fan condition	pump condition	mass flow rate (kg/s)		M_w	M_a	$M_{w\_residual}$	M_{amb_effect}
			water	air				
1	3-85%	800 rpm	0.45	2.88	14.062	8.201	0.067	0.102
2	3-60%	800 rpm	0.45	1.95	13.458	8.472	0.045	0.275
3	2-85%	800 rpm	0.45	1.92	13.931	7.208	0.038	0.287
4	2-60%	800 rpm	0.45	1.3	12.368	4.94	0.028	0.288

The provided equation (1, 2) serves as the basis for constructing a mathematical model that encompasses several key parameters, including Parameter Estimator, M_w, M_a, $M_{w\_residual}$, and M_{amb_effect}, across four distinct cases. When examining M_w, M_a, $M_{w\_residual}$, it becomes evident that lower airflow rates result in a corresponding decrease in the values of these parameters. This trend can be attributed to the roles played by M_w (representing the mass of water responsible for heat transfer) and M_a (representing the mass of air contributing to heat transfer). $M_{w\_residual}$ denotes the mass of water that remains within the pipeline. As the airflow rate decreases, the available air mass for heat exchange diminishes, consequently leading to reduced values for M_w, M_a, $M_{w\_residual}$. On the other hand, an inverse relationship is observed with M_{amb_effect} (represent the ambient air at the outlet of the radiator as induced by the fan.) in relation to airflow rate. As the airflow rate increases, M_{amb_effect} diminishes. This phenomenon arises due to the fact that higher airflow rates limit the fan's intake of ambient air that has not accumulated heat. In essence, elevated airflow rates reduce the fan's capacity to draw in cooler ambient air. As a result, the M_{amb_effect} value decreases. Conversely, lower airflow rates prompt the fan to intake a larger mass of air from the environment, which possesses less accumulated heat, leading to an increase in the M_{amb_effect} value. This can be observed in Table 1.

The airflow rate plays a pivotal role in influencing the behavior of these parameters within the mathematical model. Lower airflow rates tend to decrease the values of M_w, M_a, $M_{w\_residual}$ while increasing the value of M_{amb_effect}.

Conversely, higher airflow rates exert the opposite effect on these parameters. This observation underscores the crucial role of airflow rate in shaping the dynamics of heat transfer under investigation.

Table 2: Steady state response, water mass flow is 0.452 kg/s at 800 rpm pump condition.

Air mass flow (kg/s)	Water		Air		Q (W)	A(m^2)
	T_in (°C)	T_out (°C)	T_in (°C)	T_out (°C)		
2.88	77.15	65.49	35.67	44.12	22142.47	4.22
1.95	72.95	65.54	33.64	45.6	16373.44	3.23
1.92	83.27	76.3	35.29	47.38	13229.17	2.36
1.3	83.39	78.63	34.84	47.83	9025.19	1.77

From the Table 2, demonstrates a clear relationship between heat transfer area (A) and airflow rate, revealing a direct correlation. This connection arises because higher airflow rates result in greater temperature differences (ΔT), consequently leading to higher Q values. This relationship is mathematically represented by the heat transfer rate equation. From Fig. 1 that the heat transfer area is not uniformly distributed across the entire cross-section of the radiator.

Case 1, boasting an airflow rate of 2.88 kg/s and the operation of all three fans at 85% power, exhibits the largest heat transfer area, measuring 4.22 m^2. Conversely, Case 4, with an airflow rate of 1.3 kg/s and the activation of both fans at 60% power, demonstrates the smallest heat transfer area of 1.77 m^2. Cases 2 and 3, with airflow rates of 1.95 kg/s and 1.92 kg/s, respectively, exhibit slightly different airflow rates, resulting in distinct heat transfer areas of 3.23 m^2 and 2.36 m^2, respectively. This divergence can be attributed to the number of fans in operation. Case 2 employs three fans at 85% fan power, while Case 3 utilizes only two fans at 60% fan power. Despite their similar airflow rates, the presence of additional fans in Case 2 allows for more efficient heat exchange, leading to noticeable differences in heat transfer area.

Table 3: Experimental and modelling comparing.

case	Mass flow rate (kg/s)		Water outlet temperature (°C)			Air outlet temperature (°C)			Heat exchange rate (W)		
	Water	Air	Exp.	Sim.	%Err.	Exp.	Sim.	%Err.	Exp.	Sim.	%Err.
1	0.45	2.88	65.49	65.78	0.44	44.12	43.12	2.26	22179.37	21614.23	2.55
2	0.45	1.95	65.54	65.40	0.22	45.60	40.95	10.19	14079.90	14349.28	1.91
3	0.45	1.92	76.30	76.17	0.17	47.38	42.27	10.79	13251.22	13495.22	1.84
4	0.45	1.30	78.63	78.45	0.23	47.83	42.01	12.17	9040.23	9386.00	3.82

The Table 3 was utilized to compare the experimental and modelling values, assessing the accuracy of the created model. The water outlet temperature, with a water mass flow rate of 0.45 kg/s and an air mass flow rate of 2.88 kg/s, exhibited the highest error value at 0.44%. In contrast, the lowest error value of 0.17% was observed at a water mass flow rate of 0.45 kg/s and an air mass flow rate of 1.92 kg/s. Regarding the air outlet temperature, the highest error value, 12.17%, was recorded at a water mass flow rate of 0.45 kg/s and an air mass flow rate of 1.30 kg/s. Conversely, the lowest error value of 2.26% was registered at a water mass flow rate of 0.45 kg/s and an air mass flow rate of 2.88 kg/s.

In terms of the heat exchange rate, the greatest error value of 3.82% was observed at a water mass flow rate of 0.45 kg/s and an air mass flow rate of 1.30 kg/s, while the lowest error value, 1.84%, was noted at a water mass flow rate of 0.45 kg/s and an air mass flow rate of 1.92 kg/s. These comparisons provide insights into the model's accuracy across various conditions and highlight areas where adjustments or improvements may be needed.

From the experimental the temperature changes in the heat exchange system while controlling the water pump speed at a constant level of 800 rpm (constant water flow rate) and adjusting the airflow rate by controlling the operation of the system's fans at four different levels: 2.88 kg/s (Case 1: Turn on all fans at 85%), 1.95 kg/s (Case 2: Turn on all fans at 60%), 1.92 kg/s (Case 3: Turn on fan No. 1 & 2 at 85%), and 1.30 kg/s (Case 4: Turn on fan No. 1 & 2 at 60%), to study the results of the heat exchange system response for the radiator equipment. The results shown by the changes in the inlet water temperature (Twi), outlet water temperature (Two), inlet air temperature (Tai), and outlet air temperature (Tao) as displayed in Fig. 2.

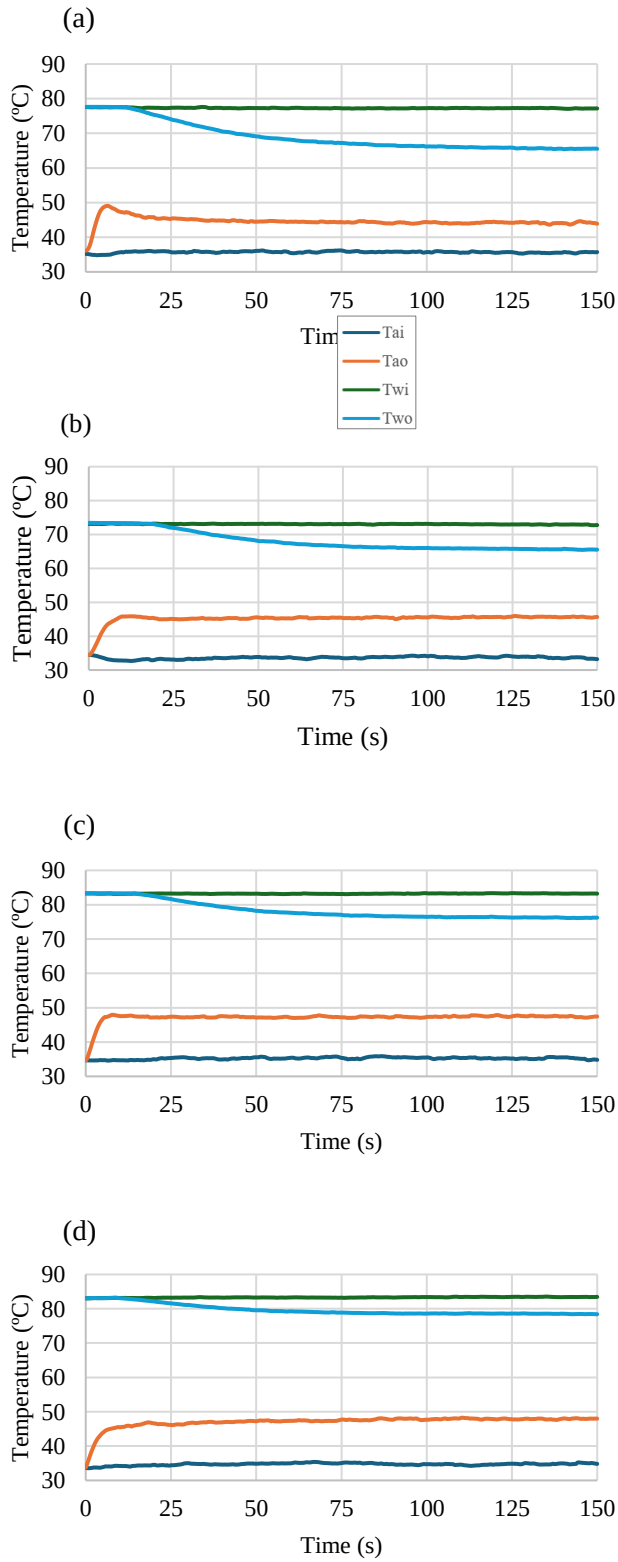

Fig. 2. The outlet temperature of cooling air and cooling water (a) Case 1: Turn On all fan at 85 % (b) Case 2: Turn On all fan at 60 % (3) Case c: Turn On fan No 1 & 2 at 85 % (4) Case d: Turn On fan No. 1 & 2 at 60 %.

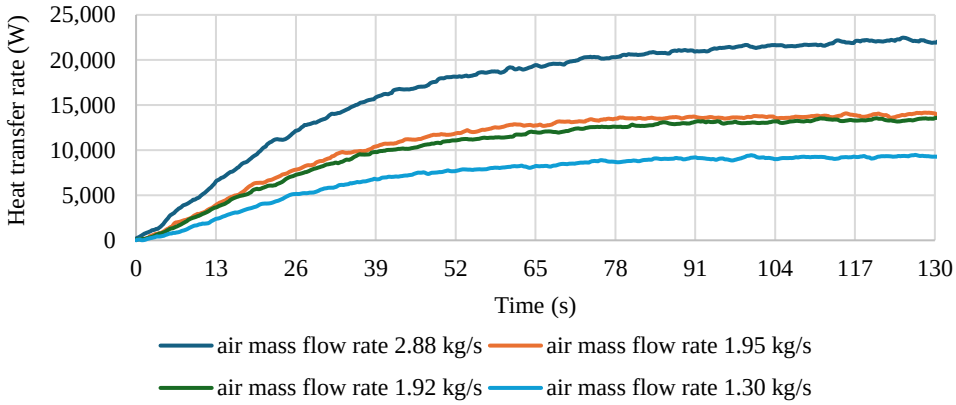

Fig. 3. The dynamic behavior of heat exchange rate.

From the test results, the temperature response parameters for the system are as follows: temperature difference of water (diff_T_w), temperature difference of air (diff_T_a), settling time duration (T_s). These parameters represent the temperature differences between various points in the system and the time it takes for the system to reach a steady-state condition. The values for these parameters are presented in Table 4.

Additionally, based on the parameters obtained from the testing, we can calculate and present the dynamic heat transfer rate of the heat exchange system as follows, dynamic heat transfer rate Fig. 3. These calculations and data will provide insights into how the heat transfer rate changes over time in the heat exchange system.

Table 4: The heat transfer rate and settling time of dynamics response of cooling system.

condition	air mass flow rate (kg/s)	settling time (s)	increasing rate of heat transfer (W/s)	Heat transfer rate (W)
Case 1	2.88	95.1	217.31	21,753.94
Case 2	1.95	85.5	152.61	13,734.94
Case 3	1.92	88.6	141.95	13,238.6
Case 4	1.30	90.2	97.36	9,244.01

4.2 Dynamic Performance and Simulation Results

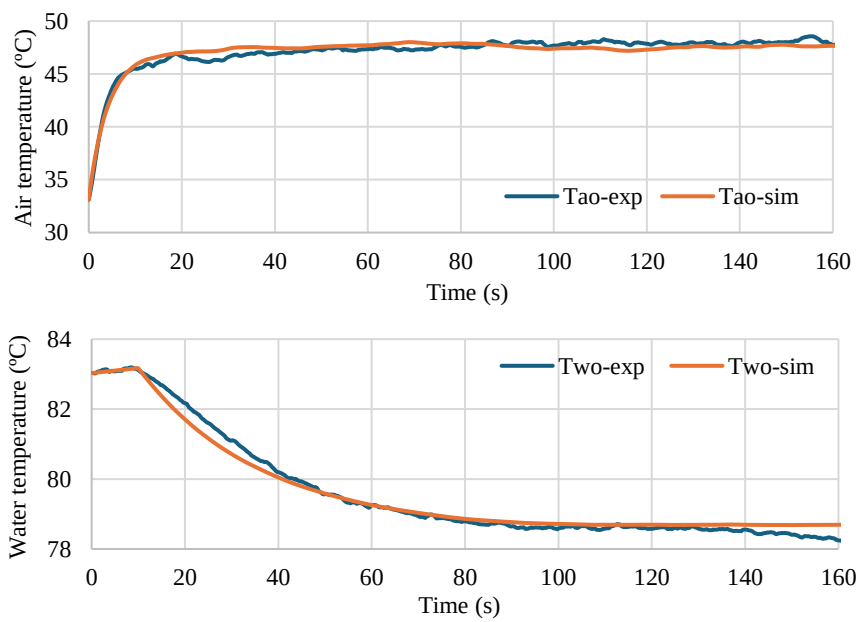

Fig. 4. The compare of outlet temperature between simulation and experimental.

The Fig. 4 presented in the upper frame of the figure illustrates the behavior of the outlet air temperature obtained from experiments, shown as a solid line, in conjunction with the temperature values predicted by the mathematical model of the system, represented by a dashed line. Both sets of data reveal that the outlet air temperature increases rapidly in the initial phase of system operation and stabilizes around the 20-second mark. Additionally, the values obtained from the model closely match the experimental results, demonstrating an acceptable level of accuracy. In the lower frame, the behavior of the cooling water temperature at the water outlet of the radiator is presented. The solid line represents the data obtained from experiments, while the dashed line represents the results from the mathematical model. The data indicates that the cooling water temperature remains relatively constant during the early moments of system operation and decreases as it approaches the 10-second mark. After that, it stabilizes and remains relatively constant until around the 80-second mark. This information highlights that both temperature changes, for air and cooling water, occur rapidly during the initial phase of system operation and then stabilize, with settling times within acceptable limits. The simulation results obtained from the mathematical model for a cooling water flow rate of 0.425 kg/s and an airflow rate of 1.3 kg/s. The RMSE of the outlet air temperature is 0.50, and the RMSE of the cooling water temperature at the water outlet is 0.21, appear to closely match the experimental data, further validating the model's reliability for the cooling system using water.

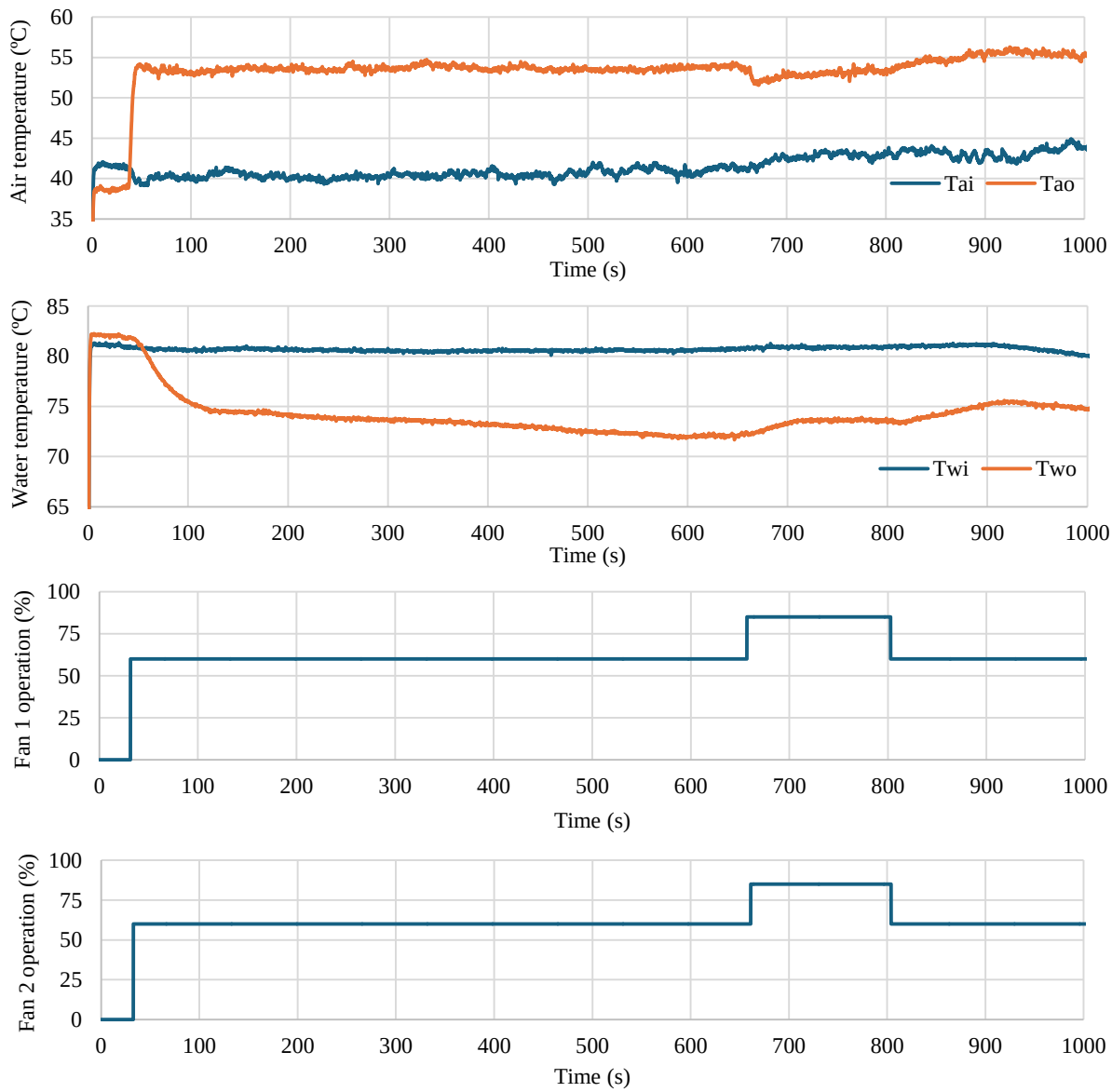

Fig. 5. The system performance with dynamic operation.

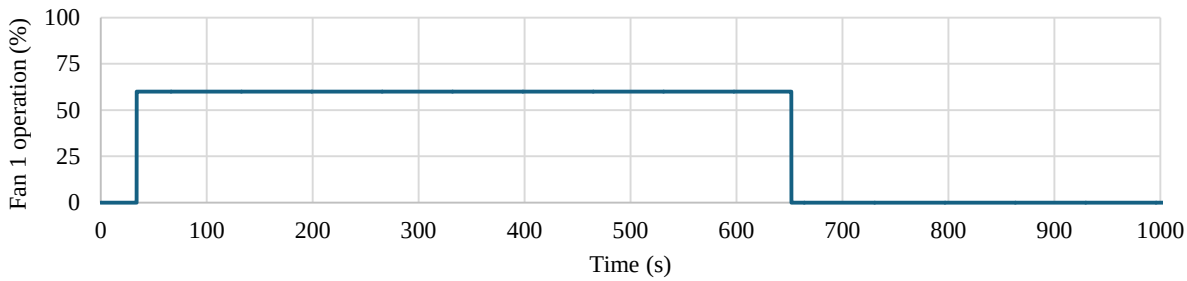

Fig. 5. (continued) The system performance with dynamic operation.

In Fig. 5, the results of testing the dynamic behavior of the heat dissipation system are presented under steady-state conditions, where the cooling water flow rate is kept constant by setting the pump's rotational speed to 800 rpm. Water is supplied at a flow rate of 0.425 kg/s, and the inlet water temperature is set at 80°C. At the 30 s., three fans are activated to dissipate air, with fan speed controlled at 60% of the maximum rotational speed. This results in an airflow rate of 1.95 kg/s. At the 650 s., the system's operation is altered by reducing the number of fans to two and increasing their rotational speed to 85% of the maximum. This leads to an airflow rate of 1.92 kg/s. At 800 s., the fan speed of the two remaining fans is further reduced to 60% of the maximum, resulting in an airflow rate of 1.3 kg/s. The system's response indicates that when the fans start operating, there is a delay in the temperature response of both the air and the cooling water. This delay time is higher for the cooling water compared to the air. Additionally, it is observed that as the airflow rate decreases, the air temperature response increases. In contrast, the airflow rate decreases when the outlet air temperature increases. These observations are evident at the 650 s. and 800 s. Furthermore, it is noted that the cooling water temperature responds with an increase in temperature as the airflow rate decreases, and it exhibits an opposite behavior when the airflow rate is increased. These observations are particularly evident at the 650 s. and 800 s. In summary, the temperature response of the air and the cooling water in the heat dissipation system exhibits delay times, and changes influence these responses in the airflow rates. The relationship between the airflow rate and temperature response is complex. It is evident in the test results at various time intervals.

5. Conclusion

This research aims to study the dynamic behavior of heat dissipation in an internal combustion engine to apply it to the cooling system of vehicles. The results indicate that the heat transfer capability is directly influenced by the flow rate of cooling water and the airflow through the radiator, as well as the temperature of the exiting cooling water, which varies with the airflow rate. It is noted that in order to achieve lower cooling water temperatures, it is necessary to increase the airflow rate through the radiator. Furthermore, the study reveals that the actual heat exchange area is affected by airflow rate in an inversely proportional manner. The cooling system's performance is influenced by the surrounding environment, as indicated by the data in Table 2, which shows diminishing effects as airflow rates increase. Additionally, the mass of water and air impacts the cooling water's thermal behavior, which varies with their respective flow rates. The air exhibits clear and distinct changes in behavior.

Acknowledgment

This research is supported by Suranaree University of Technology (SUT). The Royal Thai Navy for scholarships, and would like to thankfully acknowledge the research equipment from Cherdchai Corporation Co., Ltd.

Nomenclature

A	heat transfer surface area, m^2
c_p	specific heat of fluid, J/kg-K
D_h	hydraulic diameter, m
h	convective heat transfer coefficient, W/m^2-K
k	thermal conductivity of fluid, W/m-K
$\dot{m}$	mass flow rate, kg/s
Nu	Nusselt number

Pr	Prandtl number
Q	heat transfer rate, W
Re	Reynolds number
T	temperature, K
U	the overall heat transfer coefficient,
ρ	fluid density, kg/m^3

Subscripts

a	air
amb	ambient
ao	air outlet
c	cool
ex	exchanger
eff	effect
h	hot
i	inlet
LMD	Log Mean Difference
o	outlet
rad	radiator
res	residual
t	time
w	water

References

[1] Zhao G, Wang X, Negnevitsky M, Li C. An up-to-date review on the design improvement and optimization of the liquid-cooling battery thermal management system for electric vehicles. Appl Therm Eng. 2023;219:119626.

[2] Fonseca L, Olmeda P, Novella R, Valle RM. Internal Combustion engine heat transfer and wall temperature modeling: an overview. Arch Computat Methods Eng. 2020;27(5):1661-1679.

[3] Park S, Woo S, Kim M, Lee K. Thermal modeling in an engine cooling system to control coolant flow for fuel consumption improvement. Heat Mass Transfer. 2017;53(4):1479-1489.

[4] Banjac T, Wurzenberger JC, Katrašnik T. Assessment of engine thermal management through advanced system engineering modeling. Adv Eng Softw. 2014;71:19-33.

[5] Lu L, Chen H, Hu Y, Gong X, Zhao Z. Modeling and optimization control for an engine electrified cooling system to minimize fuel consumption. IEEE Access. 2019;7:72914-72927.

[6] Haghighat AK, Roumi S, Madani N, Bahmanpour D, Olsen MG. An intelligent cooling system and control model for improved engine thermal management. Appl Therm Eng. 2018;128:253-263.

[7] Kim KB, Choi KW, Lee KH, Lee KS. Active coolant control strategies in automotive engines. Int J Automot Technol. 2010;11:767-772.

[8] Khanjani K, Deng J, Ordys A. Controlling variable coolant temperature in internal combustion engines and its effects on fuel consumption. SAE Tech Pap. 2014:2014-32-0064.

[9] Mureșan C, Harja G. Modeling and controlling the cooling system of an IC vehicle. Int J Model Optim. 2021;11(3):80-85.

[10] Castiglione T, Pizzonia F, Bova S. A novel cooling system control strategy for internal combustion engines. SAE Int J Mater Manuf. 2016;9(2):294-302.

[11] Abdulhamitbilal E, Jafarov EM. Cooling control system with sliding mode approach for electrical vehicle with range extender. The 15th International Workshop on Variable Structure Systems (VSS); 2018 Jul 9-11; Graz, Austria. USA: IEEE; 2018. p. 267-272.

[12] Gu N, Ni JM. Simulation of engine cooling system based on AMESim. 2009 Second International Conference on Information and Computing Science; 2009 May 21-22; Manchester, UK. USA: IEEE; 2009. p. 117-120.

[13] Mohamed M, Shedid MH, El-Demerdash MS, Fatouh M. Performance of electronically controlled automotive engine cooling system using PID and LQR control techniques. IOSR-JMCE. 2018;15(3):42-51.